Available online at www.sciencedirect.com
ScienceDirect
Ceramics International 37 (2011) 2459–2465
CERAMICS INTERNATIONAL
www.elsevier.com/locate/ceramint

Mechanical properties and bioactivity of β-Ca_2SiO_4 ceramics synthesized by spark plasma sintering

Hongbin Zhong [a,b], Lianjun Wang [c,*], Yuchi Fan [a], Lingfeng He [d], Kali Lin [a], Wan Jiang [a,c,*], Jiang Chang [a], Lidong Chen [a]

[a] State Key Laboratory of High Performance Ceramics and Superfine Microstructure, Shanghai Institute of Ceramics, Chinese Academy of Sciences, Shanghai 200050, China
[b] Graduate School of the Chinese Academy of Sciences, Beijing 100049, China
[c] State Key Laboratory for Modification of Chemical Fibers and Polymer Materials, Donghua University, Shanghai 201620, China
[d] Extreme Energy-Density Research Institute, Nagaoka University of Technology, Nagaoka 940-2188, Japan

Received 27 January 2011; received in revised form 18 February 2011; accepted 28 March 2011
Available online 5 April 2011

Abstract

Bioactive beta-dicalcium silicate ceramics (β-Ca_2SiO_4) were fabricated by spark plasma sintering (SPS). The relative density of as-prepared β-Ca_2SiO_4 ceramics reached 98.1% when sintered at 1150 °C, leading to great improvement in bending strength (293 MPa), almost 10 times higher than that of the specimen prepared by conventional pressureless sintering (PLS). High fracture toughness (3.0 MPa $m^{1/2}$) and Vickers hardness (5.8 GPa) of β-Ca_2SiO_4 ceramics were also achieved by SPS at 1150 °C. The simulated body fluid (SBF) results showed that β-Ca_2SiO_4 ceramics had a good in vitro bioactivity to induce hydraxyapatite (HAp) formation on their surface, which suggests that β-Ca_2SiO_4 ceramics are promising candidates for load-bearing bone implant materials.

Keywords: A. Beta-dicalium silicate ceramics; B. Mechanical properties; C. Bioactivity; D. Spark plasma sintering

1. Introduction

Dicalcium silicate (Ca_2SiO_4) is an important material in the calcium–silica system, which is frequently identified as an important constituent in Portland cement [1,2], refractory materials [3] and corrosion-resistance coating materials [4,5]. And it has also been well studied because of its polymorphism [6]. Recently, Ca_2SiO_4 ceramics have been investigated as a new type of bioceramic for hard tissue regeneration [7,8]. Some studies [7–10] have demonstrated that Ca_2SiO_4 powders, ceramics and coatings are bioactive and can quickly induce the formation of a bone-like apatite layer on their surface after soaking in a simulated body fluid (SBF). Moreover, previous study revealed that Ca_2SiO_4 ceramics were biocompatible and could support the mesenchymal stem cells adhesion and spreading [7]. However, poor sinterability and the residual pores in Ca_2SiO_4 ceramics deteriorate the mechanical properties. Gou et al. prepared β-Ca_2SiO_4 ceramics with a relative density of only 88.8% by pressureless sintering (PLS) and the bending strength was lower than 30 MPa, which was much lower than that of the cortical bone (50–150 MPa) [7,11]. The low density resulted in the unsatisfied mechanical properties, which severely limit the application of β-Ca_2SiO_4 ceramics as load-bearing implant materials. In fact, because of the poor sinterability of silicate materials, it is still difficult to obtain fully dense β-Ca_2SiO_4 ceramics using conventional sintering techniques, such as PLS and hot-pressing (HP). Therefore, it is necessary to develop an advanced sintering technique to enhance the density and the mechanical properties of β-Ca_2SiO_4 ceramics.

Spark plasma sintering (SPS) is a well-known technique for rapid densification of various ceramics at moderate temperatures. During the SPS process, a high electric-pulsed current is applied to provide high heating rate and the activation of powder particles is considered to be achieved at short time

* Corresponding authors. Tel.: +86 21 67792835; fax: +86 21 67792855.
E-mail addresses: wanglj@dhu.edu.cn (L. Wang), wanjiang@mail.sic.ac.cn (W. Jiang).

0272-8842/$36.00.
doi:10.1016/j.ceramint.2011.03.037

[12,13]. Due to its high heating rate, high pressure, high energy activity and short sintering time, grain coarsening can be inhibited and dense ceramics with higher performance can be obtained using SPS technique at lower sintering temperatures in comparison with conventional sintering techniques (PLS, HP, etc.) [14]. Previous works showed that some bioceramics sintered by SPS, such as hydroxyapatite (HAp) and alumina (Al_2O_3), have smaller grain size and higher mechanical properties than those obtained by conventional sintering techniques [15–18].

In the present work, dense β-Ca_2SiO_4 ceramics were fabricated by the SPS technique and their mechanical properties and in vitro bioactivity were systematically investigated.

2. Materials and methods

β-Ca_2SiO_4 powders were synthesized through a modified two-step coprecipitation method using $Ca(NO_3)_2{\cdot}4H_2O$ and $Na_2SiO_3{\cdot}9H_2O$ as precursors. The synthesis process was similar to that of Ca_3SiO_5 powders [19] and not shown here for brevity. Afterwards, the β-Ca_2SiO_4 powders were sintered at 1000–1150 °C for 5 min in vacuum (<10 Pa) under a pressure of 70 MPa by spark plasma sintering (Dr. Sinter 2040, Sumitomo Coal Mining Co., Ltd., Japan).

The samples for microstructure and property characterization were cut from the as-sintered samples by a diamond wheel, polished using SiC abrasive paper and a 0.5 μm diamond suspension, respectively. The bulk density was measured by the Archimedes method. Phase identification of the as-prepared powders and ceramics was conducted via an X-ray diffractometer (XRD; D/max 2200PC, Rigaku, Japan) using monochromatic Cu Kα radiation. The fracture surfaces of the samples were observed by scanning electron microscopy (SEM; Model JSM-6700F, JEOL, Japan).

The bending strength and Young's modulus of β-Ca_2SiO_4 ceramics (2 mm × 3 mm × 18 mm) were measured using a three-point bending method in a universal testing machine (Model 1195, Instron, Canton, MA). The span length and crosshead speed were 12 mm and 0.5 mm/min, respectively. The Vickers hardness was measured with a micro-hardness tester (Tukon 2100B, Wolpert-Wilson Instrument, Aachen, Deutschland) under a load of 19.6 N and a dwell time of 15 s. The fracture toughness was determined by an indentation method described by Evans and Charles [20]. The measured values for strength, hardness and toughness were the average of 5 separate measurements.

The β-Ca_2SiO_4 ceramic discs (Φ 10 mm × 2 mm) sintered at 1150 °C were placed in polystyrene bottles containing simulated body fluid (SBF) solution (pH 7.40). The bottles with the samples and SBF were maintained at 37 °C for 1, 3, 7 and 14 days, respectively, at a surface area-to-volume ratio of 0.1 cm^2/mL without refreshing the soaking medium. The SBF was prepared as previously described by Kokubo and had similar ion concentrations to those in human blood plasma [21]. After soaking for various periods, the discs were removed from the SBF solution, rinsed with deionized water, and then dried at 60 °C. The formation of bonelike HAp on the ceramic surface was characterized by XRD, SEM and Fourier transform infrared spectroscopy (FTIR; Nicolet Co., USA) using KBr technology. The concentrations of Ca, Si and P in SBF after soaking were determined by inductively coupled plasma atomic emission spectroscopy (ICP-AES; Varian Co., USA) and pH value of the soaking solution was measured using an electrolyte-type pH meter (PHS-2C; Jingke Leici Co., China).

3. Results and discussion

3.1. Synthesis and microstructure characterization

Fig. 1 shows the XRD patterns of the as-prepared powders and bulk ceramics sintered in the range of 1000–1150 °C. All the reflections belong to β-Ca_2SiO_4, indicating that no phase evolution occurred in the SPS process.

Fig. 2 presents the SEM micrographs of fracture surfaces of β-Ca_2SiO_4 samples sintered at different temperatures. It reveals the microstructure evolution of β-Ca_2SiO_4 ceramics. When the sintering temperature was 1000 °C, the average grain size was 1–2 μm (Fig. 2(a)) and the density was 95.7% (Fig. 3). As the sintering temperature increased, pores diminished gradually, which was accompanied with the rapid increase of average grain size and density. The relative density reached 97.7% at 1050 °C. In addition, the fracture surfaces of β-Ca_2SiO_4 ceramics exhibited homogeneous microstructures composed of equiaxed grains and the average grain size increased from 1 to 2 μm at 1000 °C (Fig. 2(a)) to 2–3 μm at 1050 °C (Fig. 2(b)). As the sintering temperature reached 1100 °C, the relative density increased slightly (98.0%) while the microstructure consisted of fine equiaxed grains and large lamellar grains (Fig. 2(c)–(e)). A higher magnification image shows that the dissociation occurred along the specific crystal face even in the fine grain (Fig. 2(h)). When sintered at 1150 °C, all the fine grains grew and transformed into lamellar grains (Fig. 2(f) and (g)), while the relative density almost kept at the same level (98.1%).

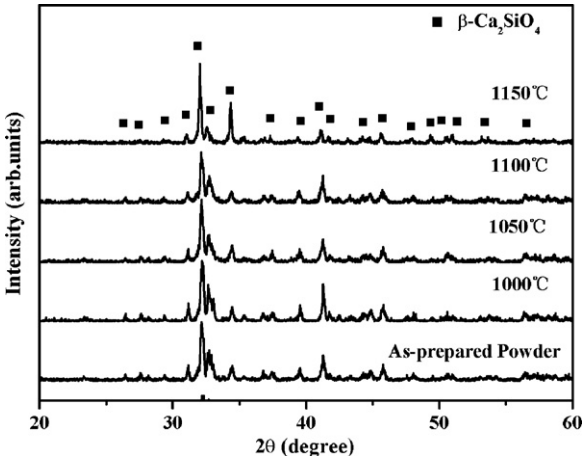

Fig. 1. XRD patterns of β-Ca_2SiO_4 powders and ceramics sintered at 1000–1150 °C.

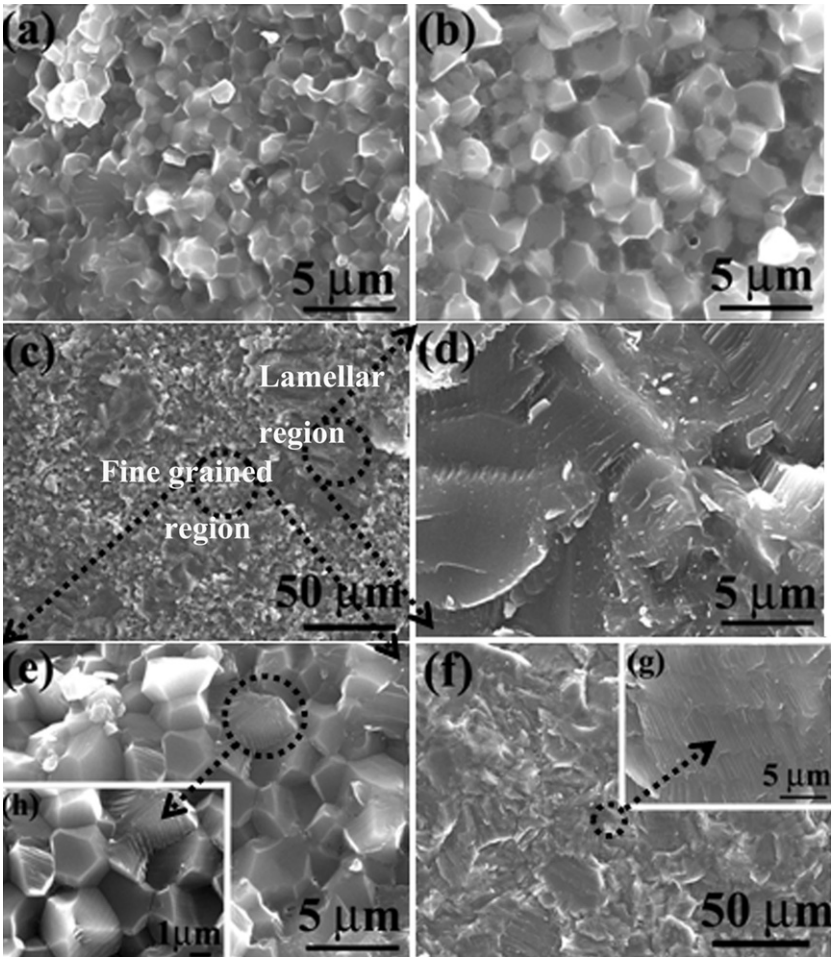

Fig. 2. SEM photographs of the fracture surface of β-Ca_2SiO_4 ceramics sintered at different temperatures: (a) 1000 °C, (b) 1050 °C, (c, d, e, h) 1100 °C and (f, g) 1150 °C.

3.2. Mechanical properties

Fig. 3 shows the influence of sintering temperature on the relative density and Vickers hardness of β-Ca_2SiO_4 ceramics. The Vickers hardness increased with the increase of sintering temperature, which was similar to the tendency of relative density. When sintered at 1000 °C, the Vickers hardness was only 4.6 GPa. At the sintering temperature of 1050 °C, the Vickers hardness increased about 14.6% (5.5 GPa). After that, the Vickers hardness of β-Ca_2SiO_4 ceramics improved slightly with the increase of the sintering temperatures. When sintered at 1150 °C, the Vickers hardness increased slightly to 5.8 GPa. The hardness reflects the local elastic and plastic deformation resistance of materials. The increase in density is in favor of hardness.

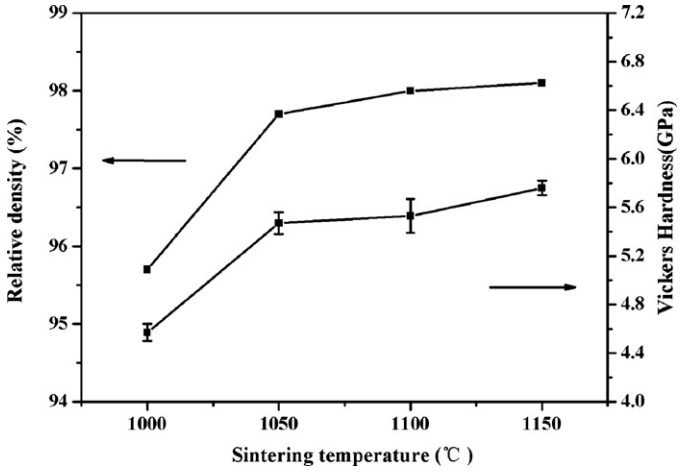

Fig. 3. The relative density and Vickers harness of β-Ca_2SiO_4 ceramics sintered at 1000–1150 °C.

The bending strength and fracture toughness of β-Ca_2SiO_4 ceramics as a function of sintering temperature are presented in Fig. 4. Both bending strength and fracture toughness increased with the sintering temperatures increasing, and the change of bending strength was more obvious. When sintered at 1000 °C, the bending strength and fracture toughness of the specimen were only 185 MPa and 2.5 MPa $m^{1/2}$, respectively. At the sintering temperature of 1150 °C, the bending strength reached the maximum value of 293 MPa, corresponding to the maximum value of Young's modulus (99 GPa). Similarly, the fracture toughness also increased with the increase of the sintering temperatures and reached the maximum value of 3.0 MPa $m^{1/2}$ when the sintering temperature was 1150 °C. The

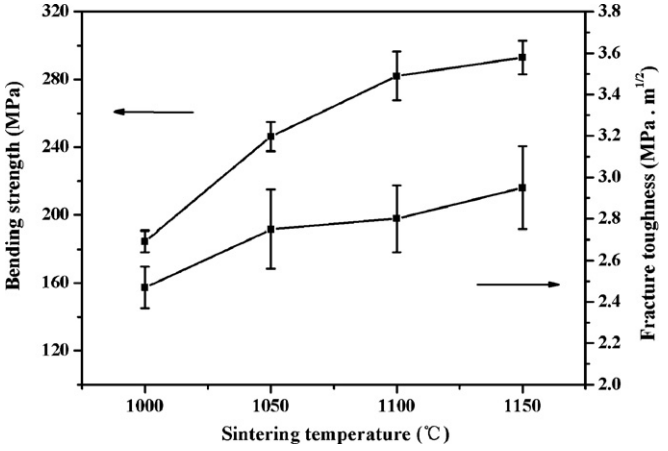

Fig. 4. Bending strength and fracture toughness vs. sintering temperature.

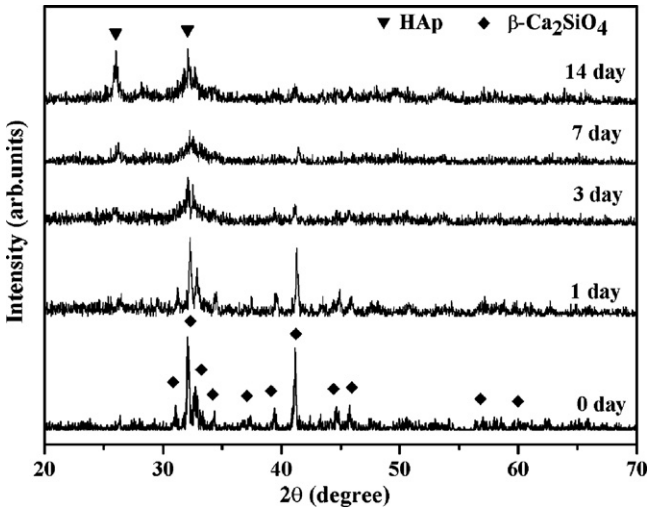

Fig. 5. XRD patterns of β-Ca_2SiO_4 ceramics before and after soaking in SBF.

increase of mechanical properties with temperature was attributed to the pore decrease and density improvement at higher sintering temperatures.

For bio-ceramics, the bending strength and fracture toughness are two crucial mechanical properties. The improvements in strength and fracture toughness are mainly associated with the increase of density, i.e. the decrease of pores. The decrease of fracture toughness is associated with flaws of specimens such as pores and cracks, which decrease the fracture energy dissipation during the fracture process. Since almost fully dense ceramics were achieved using SPS, there is no wonder that an enhancement of fracture toughness in as-prepared β-Ca_2SiO_4 ceramics was observed. At higher sintering temperature (1150 °C), improved toughness of the ceramics should also be associated with the grain morphology. The fracture surface shows the lamellar cleavage of the plate-like grains is dominant during the fracture process (Fig. 2(f)). As in the cases of Si_3N_4 [22] and SiC [23], elongated or plate-like grains promote high energy dissipation during fracture and lead to high fracture toughness. Thus, the delamination of grains may be the main reason for their relatively high fracture toughness.

It is generally accepted that the strength of ceramics improves with the increase in the density. The relative density of β-Ca_2SiO_4 ceramics sintered by SPS was higher than 98.0%. In addition, the bending strength reached 293 MPa, which was almost 10 times higher than that of the specimen obtained by PLS. This result demonstrated that SPS offers significant advantages over PLS for the consolidation of β-Ca_2SiO_4. The relative density of β-Ca_2SiO_4 ceramics consolidated by PLS was lower than 90% [7]. In addition, high temperature and long dwell time in the PLS process resulted in grain coarsening and flaw structure [24]. On the contrary, SPS is a rapid consolidation technique which includes the effects of electrical discharge, resistance heating and high pressure. All these factors could enhance densification during the SPS process.

It is known that the bioactive ceramics for the application of load-bearing sites implant and replacement are limited due to their unsatisfied mechanical properties. In this work, the bending strength of β-Ca_2SiO_4 ceramics sintered by SPS (293 MPa) was much higher than that of the cortical bone (50–150 MPa [11]). The fracture toughness of β-Ca_2SiO_4 ceramics (3.0 MPa $m^{1/2}$) was also higher than the low limit of the fracture toughness of human cortical bone (2–12 MPa $m^{1/2}$ [11]). It is necessary to fabricate β-Ca_2SiO_4 ceramics with the high fracture toughness by developing composite materials in the future.

3.3. In vitro HAp forming ability

Fig. 5 shows the XRD patterns of β-Ca_2SiO_4 ceramics before and after soaking in SBF for various periods. The intensity of β-Ca_2SiO_4 diffraction peaks decreased slightly and the peaks of HAp was not obvious after soaking for 1 day. In contrast, after a prolonged soaking time of 3 days, most diffraction peaks of β-Ca_2SiO_4 disappeared and a broad peak at $2\theta = 31.7^\circ$ corresponding to the (2 1 1) reflection of HAp was evident, indicating that the deposited HAp should be nanocrystalline. With prolonged soaking time from 3 to 14 days, the intensity of HAp peaks increased and the secondary strong peak at $2\theta = 26^\circ$ corresponding to the (0 0 2) reflection of HAp became more obvious, suggesting that more HAp deposited on the surface of ceramics.

The SEM micrographs of β-Ca_2SiO_4 ceramics soaked in SBF for different periods are presented in Fig. 6. It is evident that some nano-size crystallites and particles nucleated and deposited on the ceramic surface after soaking for 1 day (Fig. 6(a) and (b)). Some micro-cracks could also be observed on the ceramic surface caused by the shrinkage of the soaked samples in air, suggesting the formation of a thick deposition layer (Fig. 6(a)) [25]. With the increase of soaking time, more HAp agglomerates were formed and deposited on the ceramic surface and the average size of these agglomerates was about 5–8 μm (Fig. 6(c), (e) and (g)). The higher magnification SEM micrographs revealed that the agglomerates were composed of a large number of tiny worm-like crystals with typical morphology of HAp and the size of the crystallites was about 200–300 nm in length and 80 nm in diameter (Fig. 6(d), (f) and

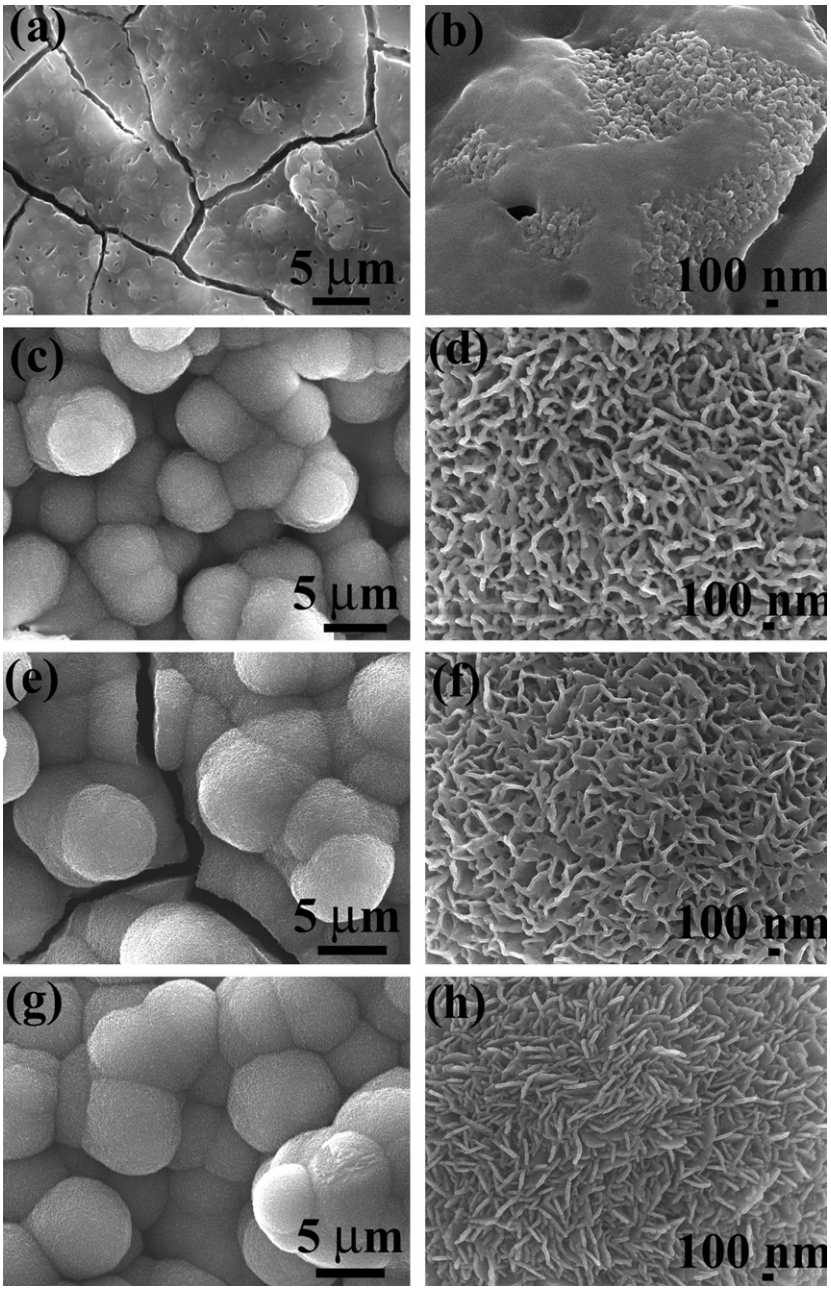

Fig. 6. SEM micrographs of β-Ca_2SiO_4 ceramics soaked in SBF for various times: (a, b) 1 day, (c, d) 3 days, (e, f) 7 days and (g, h) 14 days.

(h)). After soaking for 14 days, more HAp agglomerates grew on the ceramic surface and the HAp layer became more compact (Fig. 6(g) and (h)).

The FTIR spectra of the ceramics before and after soaking in SBF are displayed in Fig. 7. The absorption bands of silicate groups were obvious before soaking. The intense bands at 510 and 980 cm^{-1} were associated with the Si–O–Si vibrational mode of bending, and the band at 902 cm^{-1} was related to the Si–O symmetric stretch. After soaking for 1 day, the intensity of the silicate absorption bands decreased. Simultaneously, new absorption bands at 603 and 566 cm^{-1} could be detected, which were split from the P–O bending vibration (ν_4) of PO_4^{3-} group around 598 cm^{-1}. The band at 1035 cm^{-1} could be attributed to the P–O stretching vibration (ν_3) mode. All these bands were the characteristics of HAp crystals. According to the previous report of infrared correlation charts [26], it can be confirmed that HAp had formed on the ceramic surface. Furthermore, the C–O stretching of CO_3^{2-} groups at 872, 1415 and 1465 cm^{-1} and the band at 1635 cm^{-1} to the OH absorption could also be recognized in the FTIR spectra after soaking for 1 day [27]. These results further confirmed that a carbonate-containing hydroxyapatite layer could be induced to deposit on the surface of β-Ca_2SiO_4 ceramics in the SBF.

Fig. 8 presents the concentration of Ca, Si and P in SBF as well as the pH value of the immersion solutions as a function of the soaking time. It is obvious that the Ca and Si concentration increased with the soaking time increasing. Simultaneously, the pH value of the immersion solutions increased from 7.40 to

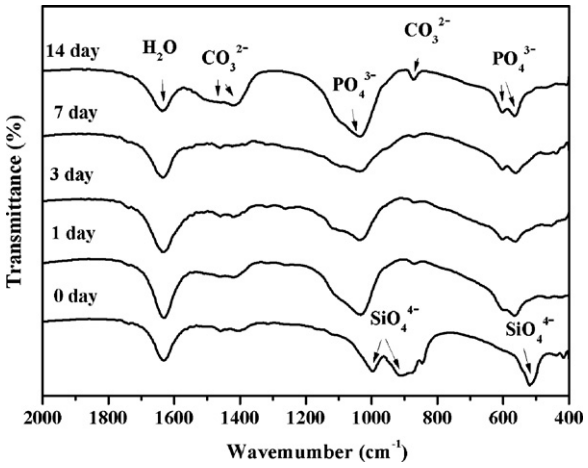

Fig. 7. FTIR spectra of β-Ca_2SiO_4 ceramics soaked in SBF for various periods.

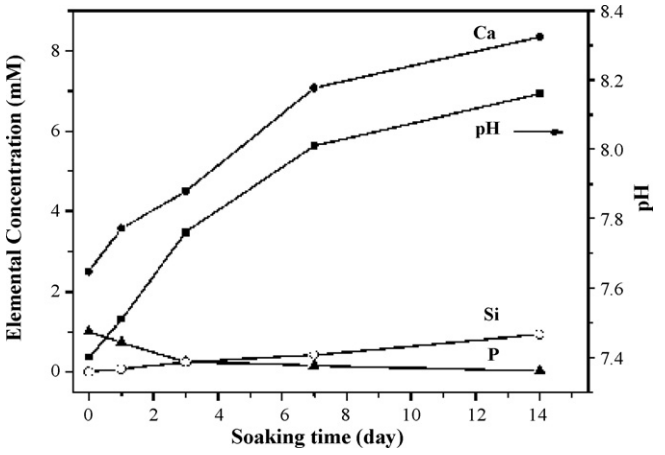

Fig. 8. Time dependence of ion concentrations and pH value in SBF solution when soaking β-Ca_2SiO_4 ceramics.

8.16 after soaking for 14 days. In contrast, the P concentration in SBF decreased steeply to a level that was only 25.5% of the starting concentration after soaking for 3 days, and then continuously decreased slowly up to 14 days. The increase in Ca and Si concentrations was attributed to the dissolution of calcium and silicate ions from β-Ca_2SiO_4 ceramics, and phosphate ions in the immersion solution were consumed with the formation of HAp, which resulted in the decrease of P concentration. Although some calcium ions were consumed to form HAp, more calcium ions were dissolved from the ceramic matrix than those were consumed. Moreover, the pH value of the resultant SBF solution increased due to the ionic exchange between calcium ions in ceramics and H^+ in SBF [28].

As we know, bioactive materials can elicit a specific biological response at the tissue–materials interface, resulting in the formation of HAp layers between the tissues and the materials. The bonelike HAp plays an essential role in forming the chemical bond of bioactive material to the living bone, and the formation of the bonelike HAp in SBF has proven to be useful in predicting the bone bonding ability of material in vitro [29]. Previous studies [11,29–31] have shown that some bioglasses and glass ceramics, including the CaO–SiO_2 components, could bond to living bone by means of forming HAp layers, and the CaO–SiO_2 components contributed mainly to the bioactivity of those materials. It has been proved that $CaSiO_3$ ceramics [32,33] and coatings [28,34] consisting of the CaO–SiO_2 components were bioactive and could induce HAp deposition when soaked in SBF. Liu et al. [28] revealed the mechanism of HAp formation on the $CaSiO_3$ surface. Firstly, calcium ions dissolved from the sample surface, leaving a hydrated silica layer, which provided favorable sites for apatite nucleation. On the other hand, the degree of supersaturation of the solution with respect to apatite increased with the dissolution of ions. Hence, the apatite nuclei were rapidly formed on the sample surface, and they spontaneously grew by consuming calcium and phosphate ions from the surrounding fluid. The composition of Ca_2SiO_4 is similar to that of $CaSiO_3$. Our results showed that β-Ca_2SiO_4 ceramics sintered by SPS also possessed excellent bioactivity and could develop a bonelike HAp layer on their surface when soaked in SBF. The ICP-AES analysis results also indicated that the mechanism of bonelike HAp formation on the surfaces of β-Ca_2SiO_4 ceramics might be similar to that of bioactive wollastonite ceramics, which corresponded well to the results of the XRD, FTIR and SEM characterizations above.

4. Conclusions

Dense β-Ca_2SiO_4 ceramics with the lamellar microsturcture were fabricated using SPS at low temperature (1150 °C). The effects of sintering temperature on the microstructures and mechanical properties were evaluated. β-Ca_2SiO_4 ceramics sintered by SPS have higher density and superior mechanical properties compared with those fabricated by PLS. The high bending strength (293 MPa), Vickers hardness (5.8 GPa), fracture toughness (3.0 MPa $m^{1/2}$) and Young's modulus (99 GPa) were achieved at 1150 °C. The bending strength of β-Ca_2SiO_4 ceramics produced by SPS was almost 10 times higher than that of the specimen obtained by PLS. The SBF soaking results revealed that β-Ca_2SiO_4 ceramics sintered by SPS had good bioactivity and could rapidly induce HAp formation after soaking in SBF. The results showed that β-Ca_2SiO_4 ceramics produced by SPS should be potential candidates as bioactive load-bearing bone repair materials.

Acknowledgements

The authors wish to thank Dr. Hong Zeng in Shanghai Institute of Ceramics for revising this manuscript. This work was funded by Shanghai Rising-Star Program (No. 09QA1406600), Shanghai Nano Science and Technology Special Project (No. 0852nm03300) and Shanghai Leading Academic Discipline Project, Project Number: B603.

References

[1] G.W. Groves, Phase-transformations in dicalcium silicate, J. Mater. Sci. 18 (6) (1983) 1615–1624.
[2] C.J. Chan, W.M. Kriven, J.F. Young, Physical stabilization of the beta-gamma transformation in dicalcium silicate, J. Am. Ceram. Soc. 75 (6) (1992) 1621–1627.

[3] J.L. Rodriguez, M.A. Rodriguez, S. De Aza, P. Pena, Reaction sintering of zircon–dolomite mixtures, J. Eur. Ceram. Soc. 21 (3) (2001) 343–354.
[4] J.W. Vogan, L. Hsu, A.R. Stetson, Thermal barrier coatings for thermal insulation and corrosion-resistance in industrial gas-turbine engines, Thin Solid Films 84 (1) (1981) 75–87.
[5] F. Jansen, X.H. Wei, M.R. Dorfman, J.A. Peters, D.R. Nagy, Performance of dicalcium silicate coatings in hot-corrosive environment, Surf. Coat. Technol. 149 (1) (2002) 57–61.
[6] D.K. Smith, A.J. Majumdar, F. Ordway, Re-examination of the polymorphism of dicalcium silicate, J. Am. Ceram. Soc. 44 (8) (1961) 405–411.
[7] Z.R. Gou, J. Chang, W.Y. Zhai, Preparation and characterization of novel bioactive dicalcium silicate ceramics, J. Eur. Ceram. Soc. 25 (9) (2005) 1507–1514.
[8] Z.R. Gou, J. Chang, W.Y. Zhai, K.L. Lin, Y. Zeng, Study on in vitro bioactivity and cytotoxicity of gamma-Ca_2SiO_4 ceramic, J. Inorg. Mater. 20 (4) (2005) 914–920.
[9] Z.G. Gou, J. Chang, Synthesis and in vitro bioactivity of dicalcium silicate powders, J. Eur. Ceram. Soc. 24 (1) (2004) 93–99.
[10] X.Y. Liu, Y.T. Xie, C.X. Ding, P.K. Chu, Early apatite deposition and osteoblast growth on plasma-sprayed dicalcium silicate coating, J. Biomed. Mater. Res. 74A (3) (2005) 356–365.
[11] L.L. Hench, Bioceramics – from concept to clinic, J. Am. Ceram. Soc. 74 (7) (1991) 1487–1510.
[12] R. Kumar, K.H. Prakash, P. Cheang, K.A. Khor, Microstructure and mechanical properties of spark plasma sintered zirconia-hydroxyapatite nano-composite powders, Acta Mater. 53 (8) (2005) 2327–2335.
[13] K.A. Khor, K.H. Cheng, L.G. Yu, F. Boey, Thermal conductivity and dielectric constant of spark plasma sintered aluminum nitride, Mater. Sci. Eng. A 347 (1–2) (2003) 300–305.
[14] L.H. Long, L.D. Chen, J. Chang, Low temperature fabrication and characterizations of beta-$CaSiO_3$ ceramics, Ceram. Int. 32 (4) (2006) 457–460.
[15] L. Gao, J.S. Hong, H. Miyamoto, S.D. De la Torre, Mechanical properties and microstructure of Al_2O_3 ceramics superfast densified by SPS, J. Inorg. Mater. 13 (6) (1998) 904–908.
[16] L. Gao, J.S. Hong, S. Torre, Bending strength and microstructure of Al_2O_3 ceramics densified by spark plasma sintering, J. Eur. Ceram. Soc. 20 (12) (2000) 2149–2152.
[17] Y.W. Gu, N.H. Loh, K.A. Khor, S.B. Tor, P. Cheang, Spark plasma sintering of hydroxyapatite powders, Biomaterials 23 (1) (2002) 37–43.
[18] Z.J. Shen, M. Johnsson, Z. Zhao, M. Nygren, Spark plasma sintering of alumina, J. Am. Ceram. Soc. 85 (8) (2002) 1921–1927.
[19] W.Y. Zhao, J. Chang, Two-step precipitation preparation and self-setting properties of tricalcium silicate, Mater. Sci. Eng. C 28 (2) (2008) 289–293.
[20] A.G. Evans, E.A. Charles, Fracture toughness determinations by indentation, J. Am. Ceram. Soc. 59 (7–8) (1976) 371–372.
[21] T. Kokubo, H. Takadama, How useful is SBF in predicting in vivo bone bioactivity? Biomaterials 27 (15) (2006) 2907–2915.
[22] F.F. Lange, Relation between strength, fracture energy, and microstructure of hot-pressed Si_3N_4, J. Am. Ceram. Soc. 56 (10) (1973) 518–522.
[23] X.F. Zhang, Q. Yang, L.C. De Jonghe, Microstructure development in hot-pressed silicon carbide: effects of aluminum, boron, and carbon additives, Acta Mater. 51 (13) (2003) 3849–3860.
[24] S.Y. Ni, L. Chou, J. Chang, Preparation and characterization of forsterite (Mg_2SiO_4) bioceramics, Ceram. Int. 33 (1) (2007) 83–88.
[25] S.Y. Ni, J. Chang, L. Chou, In vitro studies of novel CaO–SiO_2–MgO system composite bioceramics, J. Mater. Sci. – Mater. Med. 19 (1) (2008) 359–367.
[26] S.R. Radin, P. Ducheyne, Plasma spraying induced changes of calcium-phosphate ceramic characteristics and the effect on invitro stability, J. Mater. Sci. – Mater. Med. 3 (1) (1992) 33–42.
[27] S. Koutsopoulos, Synthesis and characterization of hydroxyapatite crystals: a review study on the analytical methods, J. Biomed. Mater. Res. 62 (4) (2002) 600–612.
[28] X.Y. Liu, C.X. Ding, P.K. Chu, Mechanism of apatite formation on wollastonite coatings in simulated body fluids, Biomaterials 25 (10) (2004) 1755–1761.
[29] T. Kokubo, Surface-chemistry of bioactive glass–ceramics, J. Non-Cryst. Solids 120 (1–3) (1990) 138–151.
[30] C. Ohtsuki, T. Kokubo, T. Yamamuro, Mechanism of apatite formation on CaO–SiO_2–P_2O_5 glasses in a simulated body-fluid, J. Non-Cryst. Solids 143 (1) (1992) 84–92.
[31] R. Ravarian, F. Moztarzadeh, M.S. Hashjin, S.M. Rabiee, P. Khoshakhlagh, M. Tahriri, Synthesis, characterization and bioactivity investigation of bioglass/hydroxyapatite composite, Ceram. Int. 36 (1) (2010) 291–297.
[32] K.L. Lin, J. Chang, Y. Zeng, W.J. Qian, Preparation of macroporous calcium silicate ceramics, Mater. Lett. 58 (15) (2004) 2109–2113.
[33] L.H. Long, L.D. Chen, S.Q. Bai, J. Chang, K.L. Lin, Preparation of dense beta-$CaSiO_3$ ceramic with high mechanical strength and HAp formation ability in simulated body fluid, J. Eur. Ceram. Soc. 26 (9) (2006) 1701–1706.
[34] X.Y. Liu, C.X. Ding, Z.Y. Wang, Apatite formed on the surface of plasma-sprayed wollastonite coating immersed in simulated body fluid, Biomaterials 22 (14) (2001) 2007–2012.